Journal of
Ship&Ocean
Technology
©MARCH 2004

SOTECH Vol. 8, No. 1, pp. 1 ~ 9, 2004

Experimental Investigation on the Drag Reduction for an Axi-symmetric Body by Micro-bubble and Polymer Solution

Hyun-Se Yoon[1], Young-Ha Park[1], Suak-Ho Van[1], Hyung-Tae Kim[2] and Wu-Joan Kim[3]
[1] Korea Research Institute of Ships and Ocean Engineering/KORDI, Daejeon, Korea;
E-mail: resyhs@kriso.re.kr
[2] Chungnam National University, Daejeon, Korea
[3] Mokpo National University, Mokpo, Jeonnam, Korea

Abstract

Experiments on friction drag reduction by injecting polymer (Polyethylene oxide) solution or micro-bubbles were carried out in the cavitation tunnel of KRISO. Two different drag reduction mechanisms were applied to a slender axi-symmetric body to measure the total drag reduction. And then the amount of friction drag reduction was estimated under the assumption that the reduction mechanisms were effective only to the friction drag component. As the result of the tests, polymer solution drag reduction up to 23% of the total drag was observed and it corresponds to about 35% of the estimated friction drag of the axi-symmetric body. This result matched reasonably well to that of the flat plate test "(Kim et al, 2003)". The normalization of the controlling parameters was tried at the end of this paper. Micro-bubble drag reduction was within 1% of its total drag. This unexpected result was quite different from that of the flat plate case "(Kim et al, 2003)". The possible reasons were discussed in this paper.

Keywords: drag reduction, polymer solution, micro-bubble

1 Introduction

Aiming at building a ship with better performance, naval architects have been developing or applying numerous technologies in the process of ship design. Naming a few, bulbous bow for reduction of wave resistance, hull form optimization for reduced viscous form drag by suppressing flow separation and controlling bilge vortices or applying various hull appendages for better combined resistance characteristics can be listed. However, it can be fairly said that the research on the reduction of the frictional drag itself, which is basically the major portion of the total drag, has been calling less attention so far.

The injection of micro-bubbles or polymer solutions into the turbulent boundary layer has been considered as one possibility to fit the objective. A few applications with reviews of the research in Russia, USA, Japan and EU can be found in "(proceedings on drag reduction 1998, 1999, 2001 and 2002)". It is understood that the technology has been adopted in the submarine design in USA and Russia, and some full-scale tests with the micro-bubble were conducted in Japan "(Kodama et al, 2002)". In Korea, the major ship building sector in the world, such researches are recently calling wide attention, and a few

rudimentary works "(Jang and Kim, 1999 and Kim et al, 2002)" have been performed so far.

The aim of the present work is to verify the effectiveness of the micro-bubble and the polymer solution on the reduction of frictional drag, and to obtain the key information on the controlling parameters through experiments. Drag reduction of the axi-symmetric body was investigated by varying the amount of additives and the polymer concentrations in the cavitation tunnel of KRISO.

2 Measurements of drag reduction for the axi-symmetric body

2.1 Facility and setup

2.1.1 Cavitation tunnel

The experiments were conducted in the cavitation tunnel at the Marine Transportation Systems Laboratory of the Korea Research Institute of Ships and Ocean Engineering (KRISO). The rectangular test section has dimensions of 2.6m long and 0.6m square. The maximum flow speed is 12m/s and the pressure can be varied from 0.1 to 2.0 Kgf/cm^2. The schematic sketch of the tunnel is shown in Figure 1.

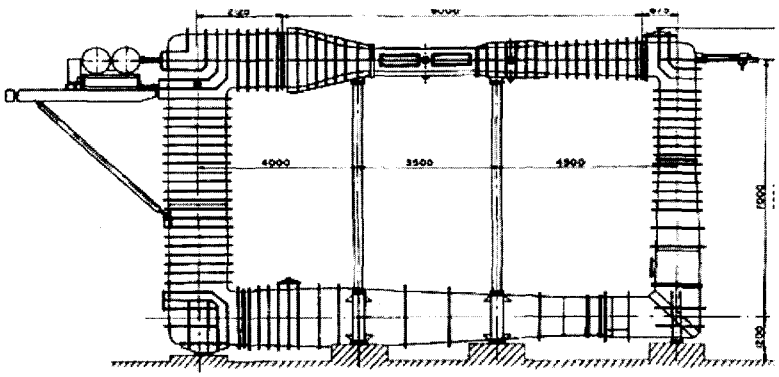

Figure 1: Schematics of the cavitation tunnel of KRISO

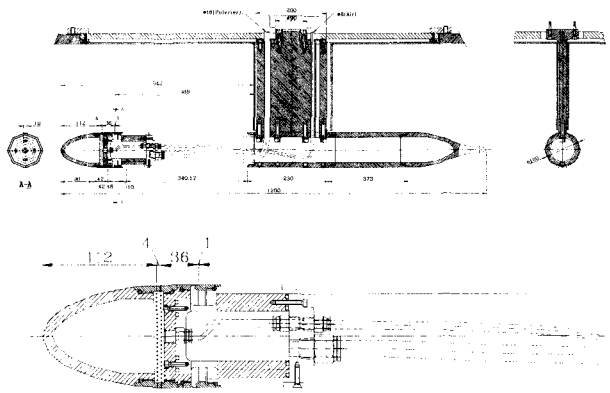

Figure 2: Schematics of the axi-symmetric body

2.1.2 Axi-symmetric body model and its installation

Figure 2 shows schematics of the axi-symmetric body. The overall length of the model is 1,200mm and its diameter is 100mm. The outline of the body is comprised of three shapes: 125mm ellipsoidal nose, 850mm parallel middle body where most skin friction drag reduction is expected and 225mm tail part expressed as a combination of a 5th order polynomial curve, a straight line and a parabola.

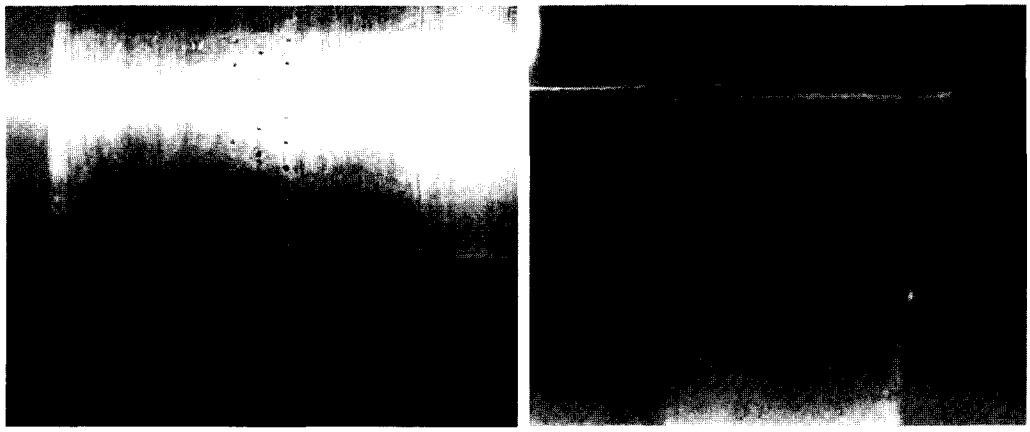

Figure 3: Photos of 0.5mm AOH(left) and polymer solution injection slot(right)

The body is supported by a rectangular shaped strut attached to the end of the total drag measurement balance. To minimize the additional drag force by the strut itself and its interaction with the body, it is enclosed with a separate and streamlined dummy strut fixed on the upper wall plate of the tunnel.

Inside the body, two separate chambers are designed for micro-bubble injection and polymer solution injection respectively. The air and the polymer solution are supplied from the outside of the tunnel through vinyl tubes passing inside the strut. At the tail part of the body a couple of small holes are deployed for filling the body with water to relieve the buoyancy force of the body exerted on the balance.

2.1.3 Micro-bubble and polymer injection units

The air is supplied from an external air compressor and contained in the air chamber inside the body. And then the air is injected circumferentially to the water flow through three staggered rows of 0.5mm diameter holes (0.5mm AOH: Array of Holes) on the body surface (Figure 3).

The polymer solution is injected by a pump consisted of a piston sliding in a cylindrical reservoir. Efficient sealing ensures that the injection flow rate is entirely governed by the rotation of a threaded rod driven through a reduction gear by an electric motor. The injection slot shown in Figure 3 is of the circular shape, which is originated from the one for the previous channel experiment. It consists of two stainless steel rings machined so that an internal circumferential gap is formed when they are assembled together. The gap between two rings is 1mm and the slot is inclined at an angle of 12.5° to the flow direction allowing polymer solutions to be injected as close and nearly tangential as possible to the wall.

The injection units are designed in such a way that the injection of micro-bubbles and polymer solution can be conducted separately or simultaneously in the experimental setup.

2.2 Test procedures

As the first step, measurements of the drag of the axi-symmetric body without injection over a range of flow speeds are necessary as a reference drag force for the analysis of the drag reduction of the body. The next step is the measurement of the drag with injecting water instead of polymer solution to measure the amount of wall jet effect itself of the injection, which would act like a thrust force to the body. Finally, drag forces were measured with injecting micro-bubbles or polymer solutions over a range of flow speed varying the injection rate of air and polymer solutions.

3 Results and discussion

3.1 Reference drag measurement and water injection

The total drag of the axi-symmetric body without injection of micro-bubbles or polymer solution was measured as a reference for the drag reduction calculation and presented in Figure 4 including the dimensionless total drag coefficients (C_T) and the friction coefficients (C_F), and those values corresponding to 7m/s and 10m/s were summarized in Table 1. The friction coefficients were calculated with the ITTC 1957 formula "(ITTC 1957)", which is a practical and common tool for naval architecture engineers.

$$C_F = \frac{R_F}{1/2\rho S V^2} = \frac{0.075}{(\log_{10} Rn - 2)^2} \tag{1}$$

Table 1: Estimation of friction drag

V (m/s)	R_{Total} (N)	R_F (N)	R_T/R_F (%)
7	40.47	26.71	66.0
10	82.75	51.15	61.8

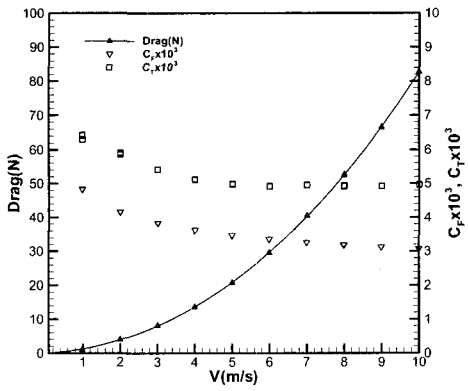

Figure 4: Total drag of the axi-symmetric body without injection

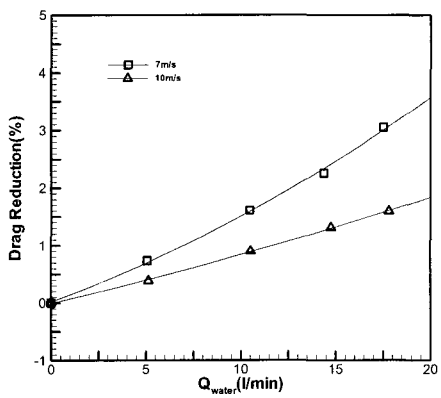

Figure 5: Wall jet effect in terms of drag reduction

For the polymer solution injection case, the additional thrust component caused by the wall jet effect should be eliminated not to overestimate the drag reducing ability of polymer solution. By injecting water instead of polymer solution the additional drag reduction could be subtracted. Figure 5 shows the measured percentile drag reduction by injection of

water at two flow speeds with varying the injection rate. Measured points are fitted to 2nd order polynomial curves to interpolate at arbitrary injection rates.

3.2 Drag reduction with O_2 gas micro-bubble injection

Figure 6 shows the reduction of the total drag, $(R_{To}-R_{Ta})/R_{To}$, in percentile at 7m/s and 10m/s flow speeds with varying the air or O_2 gas flow rate. Highly compressed O_2 gas was preferred to compressed air to supply more stable gas flow. The bulk void ratio was not measured or calculated.

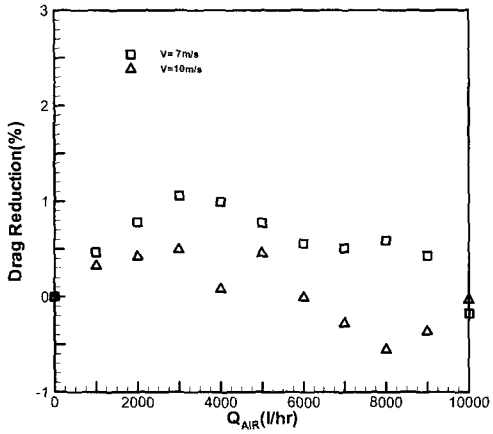

Figure 6: Total drag reduction with O_2 gas bubbles via 0.5mm AOH at 7m/s and 10m/s

For the micro-bubble injection test on the axi-symmetric body, the magnitude of maximum drag reduction does not reach that of the flat plate case at all. The maximum drag reduction was about 1% at 3,000litter/hr gas flow rate for 7m/s flow speed and even the total drag was increased over 6,000litter/hr gas flow rate for 10m/s flow speed. These values are possibly within the error bound of this test, so it might be futile to discuss about the result. The trend of those curves and the patterns of injected bubbles, however, provide some clues about why the drag reduction was so poor.

The first and most fundamental reason is that the shape of the body has no flat bottom detaining the buoyancy driven up-going bubbles differently from the flat plate cases. The second is the mechanism of bubble injection that blows the gas normal to the flow direction. The normal blowing itself induces additional drag and prevents the bubbles from staying attached to the body surface.

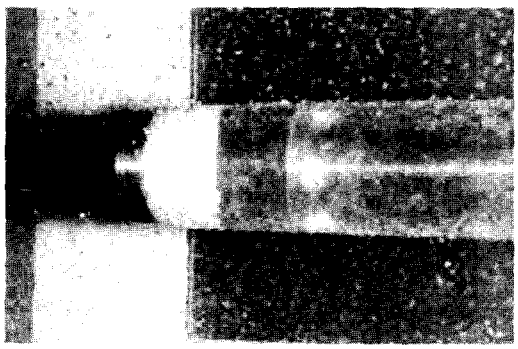

Figure 7: Photo of micro-bubble injection at 3,000litter/hr gas flow rate for 7m/s flow speed

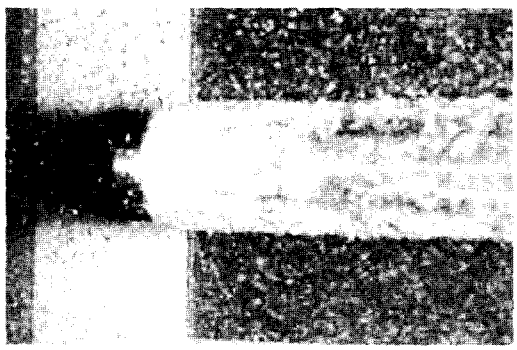

Figure 8: Photo of micro-bubble injection at 8,000litter/hr gas flow rate for 10m/s flow speed

Figure 7 shows the injected bubble pattern at 3,000litter/hr gas flow rate for 7m/s flow speed where the maximum drag reduction was obtained. Injected bubbles just behind the AOH are fairly small and well attached to the surface of the body at least near the AOH. This explains the drag reduction at small injection rate shown in Figure 6. However, since the surface area under such effect is too small the total drag reduction is not significant.

As increasing the gas flow rate, in Figure 8 for an example, injected bubbles with relatively high momentum normal to the flow become bulky to form a gas cavity, within which a flow might be trapped or retarded. The extent of this gas cavity is proportional to the injection rate. Most of the bubbles are merged into rather larger bubble clusters behind the cavity region and it is difficult to expect that such large bubbles, even away from the wall, would give any positive effect on the drag reduction. Also this inflated volume of gas cavity virtually enlarges the body volume so that the form drag increases.

To avoid this vulnerability of micro-bubble injection system, it would be advisable to try to make the injection holes with a proper angle like the polymer solution injection slot. And for a given injection rate, large number of holes with smaller diameter would reduce the momentum of bubbles normal to the flow.

3.3 Drag reduction with polymer solution injection

A flow visualization test by injecting milk instead of polymer solution was carried out precedently to verify the polymer solution injection system. The result is depicted in Figure 9. The milk flow out of the injection slot distributed quite evenly in circumferential direction and moderately injected along the body to the downstream without severe scattering or dispersion except the natural diffusion and the effect of growth of boundary layer thickness. From this result the injection of polymer solution through the designed injection slot was considered to be appropriate.

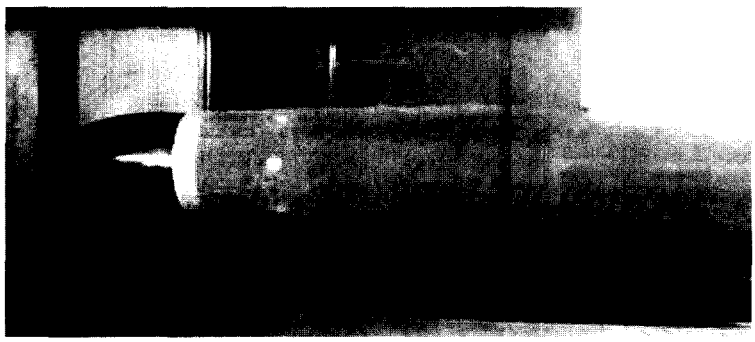

Figure 9: Photo of flow visualization with milk injection for the polymer injection test

The effect of polymer solution on drag reduction was obvious and actually prompt. From the test results, up to about 23% of total drag reduction was achieved including the corrections of the wall jet effect measured by injecting water at previous stage of this test, and this value corresponds to about 35% friction drag reduction if we accept the estimation shown in table 1. This result matches reasonably well with the result of the flat plate test[1].

Figures 10 and 11 show the effect of the injection rate of the polymer solution of two different polymer concentrations at two different flow speeds. At 7m/s flow speed, the drag reduction rates increase very rapidly as injection rate increases and becomes leveled at about 7liter/min for both 200ppm and 400ppm PEO solutions. And at 10m/s, the slopes are

relatively moderate and also become leveled at higher injection rate. The limiting injection rate seems to be pushed up for higher polymer concentration. They are about 13liter/min for the 200ppm and about 15liter/min for the 400ppm solution. For both flow speeds the higher polymer concentration show larger drag reduction.

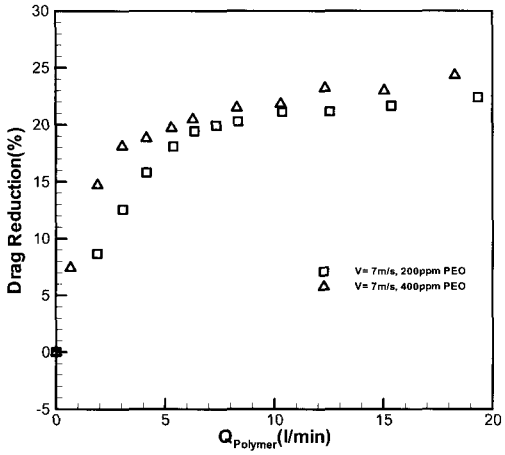

Figure 10: Comparison of total drag reduction with injection rate variation of polymer solution at 7m/s

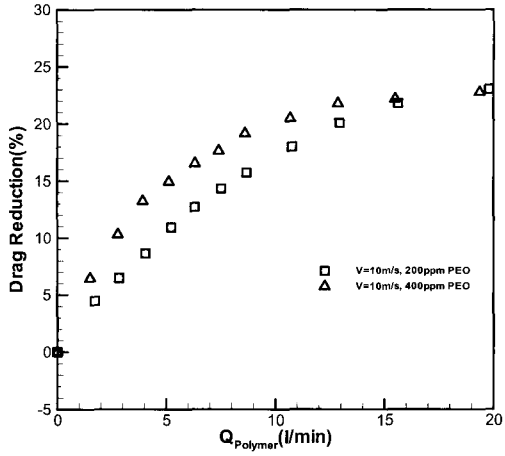

Figure 11: Comparison of total drag reduction with injection rate variation of polymer solution at 10m/s

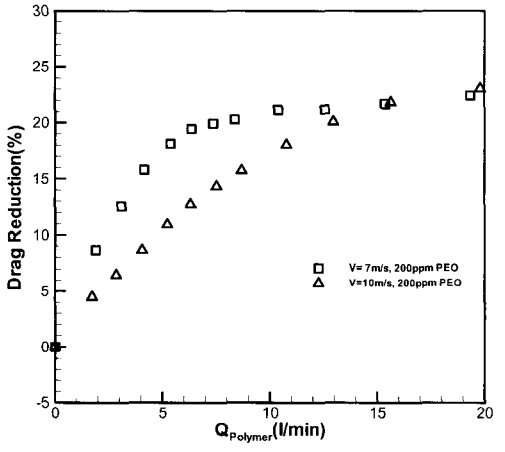

Figure 12: Comparison of total drag reduction with different flow speeds of polymer solution of 200ppm

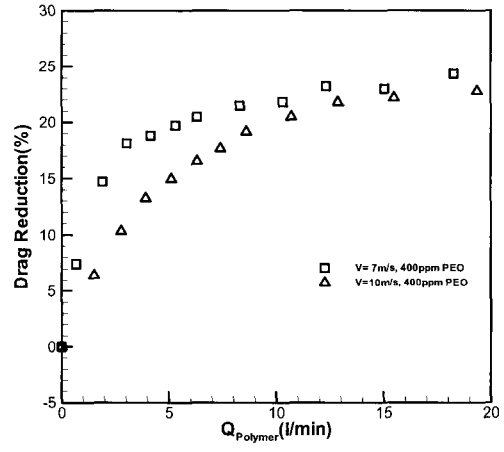

Figure 13: Comparison of total drag reduction with different flow speeds of polymer solution of 400ppm

Figures 12 and 13 are shown to see the effect of the flow speed at two fixed polymer concentrations. Curve patterns are similar each other and the slope of 7m/s is steeper than that of 10m/s for both concentrations.

All the test results are shown together in Figure 14 in a form of percentile friction drag reduction calculated under the assumption that all the drag reduction by polymer was effective only for friction drag versus normalized polymer injection rate, $Q^* = cQ_P/Q_W$, where c is the concentration of polymer solution in ppm, Q_P is polymer injection rate, and $Q_W = \pi D\delta V$ is water flow rate within the boundary layer of the body, where D is the diame-

ter of the body, δ is the boundary layer thickness, and V is the flow speed. Concerning the water flow rate, boundary layer thickness was approximated with that of a turbulent flow over a flat plate at a position corresponding to middle body. For both of Q_P and Q_W, density was ignored because their difference is considered to be negligible.

The curves in Figure 14 show somewhat similar curve patterns, but their slope and tendency to reach the maximum value are different according to flow speed and concentration of polymer solution. From this fact it could be deduced that the quantity of injected polymer, i.e. Q^*, is not directly proportional to the drag reduction, and is not a single and complete parameter to represent the polymer drag reduction phenomenon. Systematic studies and thorough understanding on polymer drag reduction mechanism would be necessary to find out more meaningful parameters.

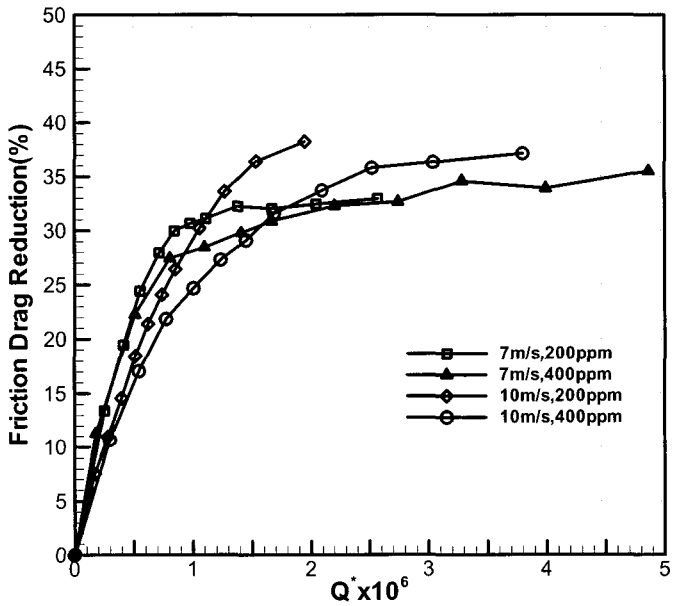

Figure 14: Comparison of friction drag reduction with normalized polymer injection rate

4 Concluding remarks

As a basic study for the development of techniques of the drag reduction of water-borne vehicles, a set of experiments on the drag reduction of an axi-symmetric body was investigated by injecting micro-bubbles of air or polymer solutions onto its surface at selective conditions. The total drag of the axi-symmetric body was measured with a 3-component balance for each of different conditions of injecting micro-bubbles, polymer solutions or pure water.

The result of the micro-bubble injection experiment was quite different from that of the flat plate test. A further study on the injection system of micro-bubble for bodies without flat bottoms would be necessary.

For the polymer solution injection, the reduction up to 23% of the total drag was observed and it corresponds to about 35% of the estimated friction drag for the axi-symmetric body. This result matched reasonably well to that of the flat plate test, and the normalization of the controlling parameters was tried.

Acknowledgment

The contents of this paper are a part of the basic research project ('Development of Key Technologies for Marine Transportation Systems', 2000-2002) of KRISO/ KORDI.

References

ITTC, Proceedings of the 8th ITTC, Madrid, Spain, published by Canal de Experiencias Hidrodinamicas, El Pardo, Madrid, 1957.

Jang, J.H. and H. Kim. 1999. On the Reduction of a Ship Resistance by Attaching an Air Cavity to Its Flat Bottom. J. of Society of Naval Architects of Korea, **36**, **2**, 1-8.

Kim, D.S, H.T. Kim and W.J. Kim. 2003. Experimental Results of Friction-Drag Reduction by Injection of Microbubbles. Proc. of the Annual Spring Meeting of Society of Naval Architecture of Korea, Chochiwon, Korea.

Kim, D.S., W.J. Kim and H.T. Kim. 2002. Experimental Study of Friction Drag Reduction in Turbulent Flow with Polymer and Microbubble Injection. Proc. of the 2nd National Congress on Fluids Engineering, 483-486.

Kim, H.T., D.S. Kim and W.J. Kim. 2003. Experimental Results of Friction-Drag Reduction by Injection of PEO Solution: Report (l). Proc. of the Annual Spring Meeting of Society of Naval Architecture of Korea, Chochiwon, Korea.

Kodama, Y., A. Kakugawa, T. Takahashi, S. Nagaya and K. Sugiyama. 2002. Microbubbles: Drag Reduction Mechanism and Applicability to Ships. 24th Symposium on Naval Hydrodynamics, Fukuoka, Japan.

Proceedings of the International Symposium on Seawater Drag Reduction, Newport, Rhode Island, 1998.

Proceedings of the 3rd Symposium on Smart Control of Turbulence, 2002 and also proceedings of the 1st and the 2nd Symposia, 1999 and 2001.